EUROPEAN ORGANIZATION FOR NUCLEAR RESEARCH

CERN-EP/98-150
21 September 1998

Single and Multi-Photon Events with Missing Energy in e^+e^- Collisions at $\sqrt{s} = 183$ GeV

The L3 Collaboration

Abstract

An analysis of single and multi-photon events with missing energy is performed using data collected with the L3 detector at LEP at centre-of-mass energies around 183 GeV, for a total of 55.3 pb^{-1} of integrated luminosity. The results obtained are in good agreement with the Standard Model prediction and are used to derive the value for the $e^+e^- \to \nu\bar{\nu}\gamma(\gamma)$ cross section as well as upper limits on cross sections of new physics processes. Several interpretations in supersymmetric models providing new limits on the masses of the lightest neutralino and of the gravitino are presented.

Submitted to *Phys. Lett. B*

1 Introduction

The increase of the centre-of-mass energy to 183 GeV achieved at LEP in 1997 offers the opportunity to search for new physics beyond the Standard Model. Single or two-photon events with missing energy could provide evidence for: pair production of neutralinos ($\tilde{\chi}^0_1\tilde{\chi}^0_1$, $\tilde{\chi}^0_1\tilde{\chi}^0_2$, $\tilde{\chi}^0_2\tilde{\chi}^0_2$, etc.) or of gravitinos ($\tilde{\mathrm{G}}\tilde{\mathrm{G}}$), for associated production of a neutralino and a gravitino ($\tilde{\chi}^0_1\tilde{\mathrm{G}}$), and for single or double production of excited neutrinos [1,2]. Neutralinos, according to different supersymmetric models, can either decay to $\tilde{\chi}^0_2 \to \tilde{\chi}^0_1\gamma$ [3] or to $\tilde{\chi}^0_1 \to \tilde{\mathrm{G}}\gamma$ [4]. The missing energy is carried away by the weakly interacting neutrino or by the lightest supersymmetric particle (LSP) which is stable under the assumption of R-parity conservation [5]. In the Minimal Supersymmetric Standard Model (MSSM [5]) with gravity mediated supersymmetry (SUSY) breaking, the LSP is the lightest neutralino ($\tilde{\chi}^0_1$). There are models, like the one proposed in Reference [6] referred to as LNZ, where the LSP is instead the gravitino. A light gravitino appears also in models with different SUSY breaking mechanisms like the Gauge Mediated SUSY Breaking (GMSB [7]).

In the Standard Model single or two-photon events with missing energy are produced via the reaction $\mathrm{e^+e^-} \to \nu\bar{\nu}\gamma(\gamma)$, which can proceed through s-channel Z exchange or t-channel W exchange. Searches for single and multi-photon final states, as well as measurements of the $\mathrm{e^+e^-} \to \nu\bar{\nu}\gamma(\gamma)$ cross section, have already been performed by L3 [8] and by other LEP experiments [9].

In the following we present a study of events with one or more photons and missing energy. Two distinct kinematic regions are considered: high energy photons from which the cross section for the $\mathrm{e^+e^-} \to \nu\bar{\nu}\gamma(\gamma)$ process is measured and low energy photons for which other Standard Model processes contribute significantly. Both regions are used in searching for new physics processes. In this paper upper limits on new physics contributions are obtained for general models as well as for supersymmetric models presented above.

2 Data Sample

In this analysis we use the data collected by the L3 detector [10] during the high energy run of LEP in 1997 corresponding to an integrated luminosity of 55.3 pb^{-1} at an average centre-of-mass energy of $\sqrt{s} = 182.7$ GeV.

Monte Carlo events for the following Standard Model processes were simulated, namely $\mathrm{e^+e^-} \to \nu\bar{\nu}\gamma(\gamma)$ with `KORALZ` [11], $\mathrm{e^+e^-} \to \gamma\gamma(\gamma)$ with `GGG` [12], Bhabha scattering for large scattering angles with `BHWIDE` [13] and for small scattering angles with `TEEGG` [14], and finally four-fermion final states specifically the processes $\mathrm{e^+e^-} \to \mathrm{e^+e^-e^+e^-}$, with `DIAG36` [15], and $\mathrm{e^+e^-} \to \mathrm{e^+e^-}\nu\bar{\nu}$ with `EXCALIBUR` [16]. The number of simulated events corresponds to more than sixty times the integrated luminosity of the collected data for all processes except Bhabha scattering and two-photon collisions for which the number is approximately five.

Signal events have been simulated with the Monte Carlo program `SUSYGEN` [17] for SUSY particle masses (M_{SUSY}) between zero and the kinematic limit and for $\Delta\mathrm{M} = M_{SUSY} - M_{LSP}$ between 1 GeV and M_{SUSY}. The t-channel exchange of a scalar electron slightly affects the angular distribution of the produced SUSY particles. For signal simulations the scalar electron ($\tilde{\mathrm{e}}_R$) mass was set to 100 GeV, except for $\tilde{\chi}^0_1\tilde{\mathrm{G}}$ production where it was set to 200 GeV.

The detector response has been fully simulated [18] for these processes.

3 Event Selection

Electrons and photons are measured in the BGO electromagnetic calorimeter. They are required to have an energy greater than 0.9 GeV, and their energy deposition pattern in the calorimeters must be consistent with an electromagnetic shower. Electrons are defined as electromagnetic clusters matched with a charged track reconstructed in the central tracking chamber. Identified conversion electrons from photons interacting with the beam pipe or with the silicon microvertex detector are also accepted as photon candidates. We define the barrel region as the polar angle range $43^\circ < \theta < 137^\circ$ with respect to the beam axis and the end-cap region as the polar angle range $14^\circ < \theta < 36^\circ$ or $144^\circ < \theta < 166^\circ$. Bhabha events and $e^+e^- \to \gamma\gamma(\gamma)$ events that are fully contained in the calorimeter are used to check the particle identification as well as the energy resolution, which is 1.2% for electrons and photons with energy greater than 5 GeV in both the barrel and the end-caps.

3.1 High Energy Photons

The selection of high energy photon candidates identifies single and multi-photon events while rejecting radiative Bhabha events and bremsstrahlung photons from out-of-time cosmic rays. The following event requirements are imposed:

- at least one photon with energy greater than 5 GeV in the barrel or end-cap region;
- the total detected energy not assigned to the identified photons smaller than 10 GeV;
- no charged tracks or exactly two charged tracks consistent with a photon conversion.

To suppress background from events with particles that are not photons, we require the energy in the hadron calorimeter to be smaller than 10 GeV. To reject cosmic ray background, we require that there be no identified muon track and no more than one BGO cluster not associated with an identified photon. For photon energies smaller than 15 GeV we require that the most energetic BGO cluster not be aligned with signals in the muon detector, while, for photon energies larger than 15 GeV, there be at least one scintillator time measurement falling within 5 ns of the beam crossing time.

To reduce the background from radiative Bhabha events, we require the energy in the SPACAL[1)] to be smaller than 7 GeV, the energy in the ALR[2)] to be smaller than 10 GeV and the energy in the luminosity monitor to be smaller than 20 GeV. Tighter cuts are applied if the transverse momentum of the event is smaller than 20 GeV and events are rejected if any energy is observed in either detector.

To further reject backgrounds from radiative Bhabha events with particles escaping along the beam pipe, as well as from the process $e^+e^- \to \gamma\gamma(\gamma)$, we also require:

- the total transverse momentum ($p_\perp$) of photons must be greater than 5 GeV;
- if two calorimetric clusters are present in opposite hemispheres their opening angle must be smaller than 3.1 rad, both in three dimensions and in the plane transverse to the beam axis.

[1)] Electromagnetic calorimeter between BGO barrel and end-caps.
[2)] Electromagnetic calorimeter between BGO end-caps and luminosity monitor.

When a second photon with an energy greater than 5 GeV is present, then the following alternative selection is applied to the two most energetic BGO clusters in order to reject the above backgrounds:

- their total transverse momentum must be greater than 3 GeV;
- if their total transverse momentum is smaller than 30 GeV we also require their acollinearity to be larger than 8.1°, their acoplanarity to be larger than 5.2°, and the missing momentum direction at least 12° away from the beam pipe;
- the recoil mass must be larger than 30 GeV.

After applying this selection we observe in the data 103 events in the barrel, with one or more photons, and 92 in the end-caps to be compared with a Monte Carlo prediction of 107.4 and 95.8 events, respectively. It consists mainly of the process $e^+e^- \to \nu\bar{\nu}\gamma(\gamma)$, with only 1.2 events expected from radiative Bhabha events, $e^+e^- \to \gamma\gamma(\gamma)$ and four-fermion processes. The observed rates of events with two photons and of photon conversions agree well with the Monte Carlo simulation. Based on studies of out-of-time events, the cosmic ray background in the event sample is estimated to be less than 1.4 events at 95% C.L.

The selection and trigger efficiency for $e^+e^- \to \nu\bar{\nu}\gamma(\gamma)$ events satisfying the kinematic requirements $E_\gamma > 5$ GeV and $\theta_\gamma > 14°$ is estimated to be $(65.4 \pm 0.3)\%$. Figure 1 shows the energy spectrum of the highest energy photon, normalized to the beam energy, for single and multi-photon events.

We observe 14 events with two photons in the data compared to the Monte Carlo prediction of 13.3 events. For recoil masses larger than 100 GeV we observe 5 events compared to an expectation of 5.6 events. Here the definition of events with two photons requires a minimum energy of the second photon of 1 GeV. Figure 2-a shows the two photon recoil mass distribution for the $\nu\bar{\nu}\gamma\gamma(\gamma)$ Monte Carlo and for the data.

3.2 Low Energy Photons

This selection extends the search for photonic final states to the low energy range. The search covers only the barrel region where a single photon trigger is implemented with a threshold at around 900 MeV [19]. We apply the following selection requirements:

- there must be only one energy deposition between 1.3 GeV and 10 GeV in the barrel region satisfying electromagnetic shape criteria;
- there must be no other BGO clusters in the barrel or end-caps, with energy greater than 200 MeV;
- the energy in the hadron calorimeter must be less than 3 GeV;
- there must be no energy deposition in the forward detectors;
- neither a track in the central tracking chamber nor a muon track is present;
- the transverse momentum of the photon must be greater than 1.3 GeV.

Specific problems at low energy are the increase of the background due to cosmic ray events and to small angle radiative Bhabha scattering, with the forward scattered electrons below the minimum tagging angle of the detector. To remove cosmic ray events we impose stringent requirements on the transverse shape of the photon shower. For the simulation of the process $e^+e^- \to e^+e^-\gamma(\gamma)$ the TEEGG [14] Monte Carlo is used, including also the fourth order contribution. It provides a reasonable simulation for photon energies larger than 1.3 GeV, even if its precision is estimated to be at the 20% level from a study of single electron events.

After applying the selection requirements we expect approximately 136 events and we observe in the data 144 events. In particular, we expect 28.2 events from the $e^+e^- \to \nu\bar{\nu}\gamma(\gamma)$ process, approximately 107 events from radiative Bhabha events and a negligible contribution from the $e^+e^- \to \gamma\gamma(\gamma)$ process. The cosmic ray background in this sample is estimated to be 1.4 ± 0.1 events. The efficiency of this selection for $\nu\bar{\nu}\gamma(\gamma)$ events in the fiducial volume defined above and satisfying the kinematic requirements (1.3 GeV $< E_\gamma <$ 10 GeV and $p_\perp >$ 1.3 GeV) is 68.6%. The trigger efficiency is included in this value. In Figure 2-b we show the observed photon energy spectrum compared to the Monte Carlo prediction.

4 $e^+e^- \to \nu\bar{\nu}\gamma(\gamma)$ Cross Section Measurement

To measure the cross section of the $e^+e^- \to \nu\bar{\nu}\gamma(\gamma)$ process we restrict the analysis to photon energies above 5 GeV. Below this value the signal to background ratio is much lower. We observe 195 events and we expect 203.2 events. Since the background contamination, for the selected energy range, is very small (0.6%) the uncertainty on the background efficiency is unimportant. The error on the measured luminosity is 0.3%.

Systematic checks similar to those described in Reference [20] have been performed. In particular the trigger simulation and the electromagnetic shower simulation are verified on data. We evaluate the efficiency loss due to cosmic ray veto requirements to be 1.1%. By means of randomly triggered beam-gate events the additional inefficiency due to noise sources not simulated in the Monte Carlo, such as that induced by beam halo in the forward detectors, is estimated to be 1.3%. A total systematic uncertainty on the efficiency of 1.6%, due to photon identification, is assigned.

The overall efficiency for the $e^+e^- \to \nu\bar{\nu}\gamma(\gamma)$ process for events satisfying the kinematic requirements $E_\gamma > 5$ GeV and $\theta_\gamma > 14^\circ$ is $65.4 \pm 0.3\ (stat) \pm 1.1\ (syst)$%. The measured cross section at $\sqrt{s} = 182.7$ GeV is:

$$\sigma_{\nu\bar{\nu}\gamma(\gamma)} = 5.36 \pm 0.39\ (stat) \pm 0.10\ (syst)\ \text{ pb.}$$

This measurement is converted into the total cross section for $e^+e^- \to \nu\bar{\nu}(\gamma)$ production of (57.7 ± 4.3) pb, to be compared to the Standard Model prediction of (60.4 ± 0.8) pb obtained with KORALZ.

5 Limits on New Physics

In the MSSM, different SUSY breaking mechanisms lead to different scenarios. All these models fulfil the requirement to have mass splittings between ordinary particles and their superpartners of at most a few TeV, but they assume very different supersymmetry breaking scales ($\sqrt{F}$). The latter, or equivalently the gravitino mass ($M_{\tilde{G}} = F/[\sqrt{3/8\pi}M_P]$ where M_P is the Planck

mass), can be considered as a free parameter. We can then distinguish three different scenarios: heavy, light and superlight gravitinos.

Usually in gravity SUSY breaking models, the gravitino is heavy (100 GeV $\lesssim M_{\tilde{\mathrm{G}}} \lesssim$ 1 TeV) and does not play a role in production or decay processes. In this scenario the single or multi photon signatures arise from one-loop decays of $\tilde{\chi}_2^0$ into $\tilde{\chi}_1^0\gamma$. This branching ratio is close to 100% if one of the two neutralinos is pure photino and the other pure higgsino.

In gauge mediated SUSY breaking models a light gravitino (10^{-2} eV $\lesssim M_{\tilde{\mathrm{G}}} \lesssim 10^2$ eV) is the LSP. In this case the gravitino plays a fundamental role in the decay of SUSY particles, in particular the $\tilde{\chi}_1^0$ is no longer stable and decays through $\tilde{\chi}_1^0 \to \tilde{\mathrm{G}}\gamma$ (for $M_{\tilde{\chi}_1^0} < M_{\mathrm{Z}}$).

When the gravitino is superlight (10^{-6} eV $\lesssim M_{\tilde{\mathrm{G}}} \lesssim 10^{-4}$ eV) it can be produced abundantly not only in SUSY particle decays but also directly in pairs or associated to a neutralino.

The selections described in this paper are devised for photons originating from the interaction point. For neutralino mean decay length larger than 1 cm the experimental sensitivity drops. This problem can arise only for peculiar situations in the light gravitino scenario. For instance for $M_{\tilde{\chi}_1^0} = 10$ GeV and $M_{\tilde{\mathrm{G}}} = 1$ eV, the decay length is approximately 10^3 cm. In the following all limits in the gravitino LSP scenario are under the assumption of $d_{\tilde{\chi}_1^0} < 1$ cm.

5.1 Single photon

We first consider the general process $\mathrm{e^+e^-} \to \mathrm{XY} \to \mathrm{XX}\gamma$, with $\mathrm{M}_Y > \mathrm{M}_X$. To derive cross section limits for specific M_X and M_Y pairings, we impose the requirement (additional to those described in sections 3.1 and 3.2) that the most energetic photon in the event has an energy kinematically consistent with the assumed M_Y and M_X. Since isotropic photon production is assumed, we restrict the photon candidates to the barrel region. Figure 3 shows the resulting 95% C.L. upper limits on the cross sections for the process $\mathrm{e^+e^-} \to \mathrm{XY} \to \mathrm{XX}\gamma$.

For interpretations within the MSSM framework we do not impose the additional requirement on the photon energy. Moreover we do not a priori restrict the fiducial region, since the t-channel production is often important and the rate of photons in the end-caps may be enhanced. Instead a likelihood approach [21] is adopted and the photon energy spectra for data, background and signal simulations are compared in order to get the 95% C.L. upper limit on new physics cross sections.

5.1.1 Heavy Gravitino

In this scenario the single photon signature arises from the reaction $\mathrm{e^+e^-} \to \tilde{\chi}_2^0\tilde{\chi}_1^0$, which proceeds through s-channel Z exchange and t-channel scalar electron exchange ($\tilde{\mathrm{e}}_{R,L}$). The one-loop decay $\tilde{\chi}_2^0 \to \tilde{\chi}_1^0\gamma$ is the dominant channel only in peculiar regions of the parameter space in the MSSM with GUT assumptions [22]. However, if the relation between the soft SUSY breaking parameters M_1 and M_2 is relaxed this decay can occur for any $\tilde{\chi}_2^0$–$\tilde{\chi}_1^0$ mass combination.

Typical efficiencies for this process are around 75%. We use our single photon spectrum (Figures 1-a and 2-b) to set cross section upper limits for the reaction $\mathrm{e^+e^-} \to \tilde{\chi}_2^0\tilde{\chi}_1^0$ (Figure 4-a) under the assumption of 100% branching ratio for $\tilde{\chi}_2^0 \to \tilde{\chi}_1^0\gamma$.

5.1.2 Superlight Gravitino

In the LNZ model [6] the gravitino is superlight and the neutralino is the next to lightest SUSY particle. The reaction $\mathrm{e^+e^-} \to \tilde{\mathrm{G}}\tilde{\chi}_1^0$, which proceeds through s-channel Z exchange and t-channel

$\tilde{e}_{R,L}$ exchange, has sizeable cross sections. The $\tilde{\chi}_1^0$ composition is almost pure bino; this leads to the dominant decay channel $\tilde{\chi}_1^0 \to \tilde{G}\gamma$, but for $M_{\tilde{\chi}_1^0} \gtrsim 100$ GeV the decay into Z is not negligible.

Efficiencies for this process range between 63% for $M_{\tilde{\chi}_1^0} = 0.5$ GeV and 77% for $M_{\tilde{\chi}_1^0}$ at the kinematic limit. The cross section upper limit as a function of $M_{\tilde{\chi}_1^0}$ is shown in Figure 4-b together with the average limit obtained with Monte Carlo experiments with background only. The probability to obtain a better limit in the background-only hypothesis is at least 20% for all neutralino mass hypotheses.

In the LNZ model there are only two free parameters, the gravitino and the neutralino masses. Exclusions in the model are then completely specified in the plane $M_{\tilde{G}} - M_{\tilde{\chi}_1^0}$ as shown for our result in Figure 5-a.

In supersymmetric models with superlight gravitinos also the process $e^+e^- \to \tilde{G}\tilde{G}$ can be relevant [23]. If $M_{\tilde{\chi}_1^0} > \sqrt{s}$ this is the only accessible reaction to produce SUSY particles. When accompanied by initial state radiation this reaction leads to single or multi photon signatures. In this scenario the energy spectrum of photons is the usual exponentially falling, but without the peak of the "return-to-the-Z". In addition, other diagrams contributing to the $\tilde{G}\tilde{G}\gamma(\gamma)$ final state extend the spectrum to high energies but at a rate significantly lower. A Monte Carlo program based on formulas in Reference [23], which takes into account the emission of only one photon, has been used to estimate the selection efficiency. From the likelihood fit to the observed energy spectrum we derive the lower limit on the SUSY breaking scale, which is set at 95% C.L. to $\sqrt{F} > 182.5$ GeV and consequently for the gravitino mass:

$$M_{\tilde{G}} > 7.9 \cdot 10^{-6} \text{ eV}.$$

The observed exclusion confidence level and the average confidence level obtained with Monte Carlo experiments with background only, are shown as a function of the gravitino mass in Figure 5-b. The probability to observe a higher limit than the one actually measured is 26%.

5.2 Multi photon

For the multi photon final state two different scenarios are possible in supersymmetric models: the neutralino LSP scenario ($\tilde{\chi}_2^0\tilde{\chi}_2^0 \to \tilde{\chi}_1^0\gamma\tilde{\chi}_1^0\gamma$) and the gravitino LSP scenario ($\tilde{\chi}_1^0\tilde{\chi}_1^0 \to \tilde{G}\gamma\tilde{G}\gamma$). In both scenarios observable rates of events with two photons and missing energy are foreseen at e^+e^- colliders.

For detection of processes with multiple photons a different approach is adopted, with respect to the single photon case. We reduce completely the $e^+e^- \to \nu\bar{\nu}\gamma\gamma(\gamma)$ background by means of additional cuts on the energy and on the angle with respect to the beam axis of the photons. These cuts are optimized for each mass point separately, maximizing the sensitivity function also used in Reference [24].

5.2.1 Heavy Gravitino

The reaction $e^+e^- \to \tilde{\chi}_2^0\tilde{\chi}_2^0$ proceeds through s-channel Z exchange and t-channel $\tilde{e}_{R,L}$ exchange. Typical efficiencies for this process are around 60%. The accepted background and selected data vary, according to the $\tilde{\chi}_2^0$ and $\tilde{\chi}_1^0$ mass hypotheses, in a range between 0.05 expected background events, with no data selected, and 2.8 expected background events, with 3 events selected in data. Cross section upper limits at 95% C.L. are obtained as shown in Figure 6-a.

The results shown in Figure 6-a and those in Figure 4-a are combined and an exclusion in terms of limits on the MSSM parameters, with GUT assumptions [22], is obtained. The limits

$M_{\tilde{\chi}_1^0}$(GeV)	Eff.(%)	Backgr.	Data	σ_{95}(pb)
91	68.4	0.13	0	0.079
85	66.0	0.50	0	0.082
80	63.6	0.86	0	0.085
75	60.6	0.71	0	0.089
70	55.4	0.73	0	0.098
60	52.6	1.19	0	0.103
45	44.0	0.94	0	0.123
30	42.2	0.83	0	0.128
15	40.8	0.97	0	0.133
0.5	41.4	1.24	1	0.176

Table 1: Efficiencies, number of expected background and selected data events, and 95% C.L. upper limits for the process $e^+e^- \to \tilde{\chi}_1^0\tilde{\chi}_1^0 \to \tilde{G}\tilde{G}\gamma\gamma$ for various $\tilde{\chi}_1^0$ masses.

on $\tilde{\chi}_2^0\tilde{\chi}_2^0$ and $\tilde{\chi}_2^0\tilde{\chi}_1^0$ productions lead to an excluded region in the $M_2 - \mu$ plane as shown in Figure 6-b[3]. This exclusion combined with dedicated searches for charginos, neutralinos and scalar leptons [24], is useful to improve the indirect limit on the lightest neutralino mass.

5.2.2 Light Gravitino

Typical efficiencies for the process $e^+e^- \to \tilde{\chi}_1^0\tilde{\chi}_1^0 \to \tilde{G}\tilde{G}\gamma\gamma$ are shown in Table 1 together with the expected background and selected data. In the last column the 95% C.L. upper limit on the production cross section is shown. The derived cross section limits at 95% C.L. are plotted in Figure 7-a versus the neutralino mass. The theoretical prediction for three extreme cases of neutralino composition[4] [25], which determines its coupling to the photon and to the Z, are plotted in the same Figure. In GMSB models the neutralino is almost pure bino, we can then derive in these models lower limits on the mass of the lightest neutralino between 79 GeV and 84 GeV for $M_{\tilde{e}_{R,L}}$ between 150 GeV and 100 GeV respectively.

Limits on the MSSM parameters can also be obtained. In particular in the light gravitino scenario the cross section limits on $\tilde{\chi}_1^0\tilde{\chi}_1^0$ production are translated into excluded regions in the $M_2 - \mu$ plane as shown in Figure 7-b.

Figure 8 shows the exclusion at 95% C.L., in the $\tilde{\chi}_1^0 - \tilde{e}$ mass plane, derived with our data. This exclusion obtained within the framework of the GMSB model is confronted to the SUSY interpretation of the event $e^+e^-\gamma\gamma$ and transverse missing energy observed by CDF [26]. This event, which can hardly be assigned to Standard Model processes, has a natural interpretation in supersymmetric models preferentially in the scalar electron scenario with gravitino LSP. The kinematics of this event is consistent only with a limited set of $\tilde{\chi}_1^0 - \tilde{e}$ mass combinations [25]. In Figure 8 the 95% C.L. exclusion almost rules out the SUSY interpretation of the CDF event.

[3] M_2 is the SU(2) gaugino mass parameter, μ the Higgs-mixing mass, $\tan\beta$ the ratio of the vacuum expectation values of the two Higgs doublets and m_0 the common mass for scalar fermions at the GUT scale.

[4] For the Higgsino case a 2% photino component is required to ensure the decay into $\gamma\tilde{G}$.

6 Acknowledgements

We wish to congratulate the CERN accelerator divisions for the successful upgrade of the LEP machine and to express our gratitude for its good performance. We acknowledge with appreciation the effort of all engineers, technicians and support staff who have participated in the construction and maintenance of this experiment.

References

[1] F. Boudjema *et al.*, in "Z Physics at LEP 1", CERN Report CERN 89-08, eds. G. Altarelli, R. Kleiss and C. Verzegnassi (CERN, Geneva, 1989) Vol. 2, p. 188 and references therein.

[2] K. Hagiwara *et al.*, Z. Phys. **C 29** (1985) 115.

[3] P. Fayet, Phys. Lett. **B 117** (1982) 460;
H.E. Haber and D. Wyler, Nucl. Phys. **B 323** (1989) 267;
S. Ambrosanio and B. Mele, Phys. Rev. **D 53** (1996) 2541;
S. Ambrosanio *et al.*, Phys. Rev. Lett. **76** (1996) 3498.

[4] J. Ellis and J.S. Hagelin, Phys. Lett. **B 122** (1983) 303;
J. Ellis *et al.*, Phys. Lett. **B 147** (1984) 99;
P. Fayet , Phys. Lett. **B 175** (1986) 471;
S. Dimopoulos *et al.*, Phys. Rev. Lett. **76** (1996) 3494;
D.R. Stump *et al.*, Phys. Rev. **D 54** (1996) 1936.

[5] Y.A. Golfand and E.P. Likhtman, Sov. Phys. JETP **13** (1971) 323;
D.V. Volkhov and V.P. Akulov, Phys. Lett. **B 46** (1973) 109;
J. Wess and B. Zumino, Nucl. Phys. **B 70** (1974) 39;
P. Fayet and S. Ferrara, Phys. Rep. **C 32** (1977) 249;
A. Salam and J. Strathdee, Fortschr. Phys. **26** (1978) 57.

[6] J.L. Lopez, D.V. Nanopoulos and A. Zichichi, Phys. Rev. **D 55** (1997) 5813.

[7] See for instance:
C. Kolda, Nucl. Phys. Proc. Suppl. **62** (1998) 266.

[8] L3 Collab., M. Acciarri *et al.*, Phys. Lett. **B 415** (1997) 299;
L3 Collab., M. Acciarri *et al.*, Phys. Lett. **B 431** (1998) 199.

[9] ALEPH Collab., D. Buskulic *et al.*, Phys. Lett. **B 313** (1993) 520;
ALEPH Collab., R. Barate *et al.*, Phys. Lett. **B 429** (1998) 201;
DELPHI Collab., P. Abreu *et al.*, Phys. Lett. **B 380** (1996) 471;
DELPHI Collab., P. Abreu *et al.*, Z. Phys. **C 74** (1997) 577;
OPAL Collab., R. Akers *et al.*, Z. Phys. **C 65** (1995) 47;
OPAL Collab., K. Ackerstaff *et al.*, Eur. Phys. Journal **C 2** (1998) 607.

[10] L3 Collab., B. Adeva *et al.*, Nucl. Instr. and Meth. **A 289** (1990) 35;
M. Chemarin *et al.*, Nucl. Instr. and Meth. **A 349** (1994) 345;
M. Acciarri *et al.*, Nucl. Instr. and Meth. **A 351** (1994) 300;
G. Basti *et al.*, Nucl. Instr. and Meth. **A 374** (1996) 293;

I.C. Brock *et al.*, Nucl. Instr. and Meth. **A 381** (1996) 236;
A. Adam *et al.*, Nucl. Instr. and Meth. **A 383** (1996) 342.

[11] The KORALZ version 4.02 is used.
S. Jadach, B.F.L. Ward and Z. Wąs, Comp. Phys. Comm. **79** (1994) 503.

[12] F.A. Berends and R. Kleiss, Nucl. Phys. **B 186** (1981) 22.

[13] S. Jadach *et al.*, Phys. Lett. **B 390** (1997) 298.

[14] The TEEGG version 7.1 is used.
D. Karlen, Nucl. Phys. **B 289** (1987) 23.

[15] F.A. Berends, P.H. Daverfeldt and R. Kleiss, Nucl. Phys. **B 253** (1985) 441.

[16] F.A. Berends, R. Kleiss and R. Pittau, Nucl. Phys. **B 424** (1994) 308; Nucl. Phys. **B 426** (1994) 344; Nucl. Phys. (Proc. Suppl.) **B 37** (1994) 163; Phys. Lett. **B 335** (1994) 490; Comp. Phys. Comm. **83** (1994) 141.

[17] SUSYGEN version 2.2 is used. S. Katsanevas and P. Morawitz, E-preprint hep-ph/9711417. Submitted to Comp. Phys. Comm.

[18] The L3 detector simulation is based on GEANT Version 3.15.
See R. Brun *et al.*, "GEANT 3", CERN DD/EE/84-1 (Revised), September 1987.
The GHEISHA program (H. Fesefeldt, RWTH Aachen Report PITHA 85/02 (1985)) is used to simulate hadronic interactions.

[19] R. Bizzarri *et al.*, Nucl. Inst. Meth. **A 317** (1992) 463.

[20] L3 Collab., M. Acciarri *et al.*, Phys. Lett. **B 415** (1997) 299.

[21] A. Favara and M. Pieri, "Confidence level estimation and analysis optimisation", preprint DFF-278/4/1997, E-preprint hep-ex 9706016.

[22] See for instance:
L. Ibanez, Phys. Lett. **B 118** (1982) 73;
R. Barbieri, S. Farrara and C. Savoy, Phys. Lett. **B 119** (1982) 343.

[23] A. Brignole, F. Feruglio and F. Zwirner, Nucl. Phys. **B 516** (1998) 13.

[24] L3 Collab., M. Acciarri *et al.*, Eur. Phys. Journal **C 4** (1998) 207.

[25] J.L. Lopez and D.V. Nanopoulos, Phys. Rev. **D 55** (1997) 4450.

[26] CDF Collab., F. Abe *et al.*, FERMILAB-PUB-98-024-E, Submitted to Phys. Rev. Lett.

The L3 Collaboration:

M.Acciarri,[28] O.Adriani,[17] M.Aguilar-Benitez,[27] S.Ahlen,[12] J.Alcaraz,[27] G.Alemanni,[23] J.Allaby,[18] A.Aloisio,[30] M.G.Alviggi,[30] G.Ambrosi,[20] H.Anderhub,[49] V.P.Andreev,[7,38] T.Angelescu,[14] F.Anselmo,[10] A.Arefiev,[29] T.Azemoon,[3] T.Aziz,[11] P.Bagnaia,[37] L.Baksay,[44] S.Banerjee,[11] Sw.Banerjee,[11] K.Banicz,[46] A.Barczyk,[49,47] R.Barillère,[18] L.Barone,[37] P.Bartalini,[23] A.Baschirotto,[28] M.Basile,[10] R.Battiston,[34] A.Bay,[23] F.Becattini,[17] U.Becker,[16] F.Behner,[49] J.Berdugo,[27] P.Berges,[16] B.Bertucci,[34] B.L.Betev,[49] S.Bhattacharya,[11] M.Biasini,[34] A.Biland,[49] G.M.Bilei,[34] J.J.Blaising,[4] S.C.Blyth,[35] G.J.Bobbink,[2] R.Bock,[1] A.Böhm,[1] L.Boldizsar,[15] B.Borgia,[18,37] D.Bourilkov,[49] M.Bourquin,[20] S.Braccini,[20] J.G.Branson,[40] V.Brigljevic,[49] I.C.Brock,[35] A.Buffini,[17] A.Buijs,[45] J.D.Burger,[16] W.J.Burger,[34] J.Busenitz,[44] A.Button,[3] X.D.Cai,[16] M.Campanelli,[49] M.Capell,[16] G.Cara Romeo,[10] G.Carlino,[30] A.M.Cartacci,[17] J.Casaus,[27] G.Castellini,[17] F.Cavallari,[37] N.Cavallo,[30] C.Cecchi,[20] M.Cerrada,[27] F.Cesaroni,[24] M.Chamizo,[27] Y.H.Chang,[51] U.K.Chaturvedi,[19] M.Chemarin,[26] A.Chen,[51] G.Chen,[8] G.M.Chen,[8] H.F.Chen,[21] H.S.Chen,[8] X.Chereau,[4] G.Chiefari,[30] C.Y.Chien,[5] L.Cifarelli,[39] F.Cindolo,[10] C.Civinini,[17] I.Clare,[16] R.Clare,[16] G.Coignet,[4] A.P.Colijn,[2] N.Colino,[27] S.Costantini,[9] F.Cotorobai,[14] B.de la Cruz,[27] A.Csilling,[15] T.S.Dai,[16] R.D'Alessandro,[17] R.de Asmundis,[30] A.Degré,[4] K.Deiters,[47] D.della Volpe,[30] P.Denes,[36] F.DeNotaristefani,[37] M.Diemoz,[37] D.van Dierendonck,[2] F.Di Lodovico,[49] C.Dionisi,[18,37] M.Dittmar,[49] A.Dominguez,[40] A.Doria,[30] M.T.Dova,[19,♯] D.Duchesneau,[4] P.Duinker,[2] I.Duran,[41] S.Easo,[34] H.El Mamouni,[26] A.Engler,[35] F.J.Eppling,[16] F.C.Erné,[2] P.Extermann,[20] M.Fabre,[47] R.Faccini,[37] M.A.Falagan,[27] S.Falciano,[37] A.Favara,[17] J.Fay,[26] O.Fedin,[38] M.Felcini,[49] T.Ferguson,[35] F.Ferroni,[37] H.Fesefeldt,[1] E.Fiandrini,[34] J.H.Field,[20] F.Filthaut,[18] P.H.Fisher,[16] I.Fisk,[40] G.Forconi,[16] L.Fredj,[20] K.Freudenreich,[49] C.Furetta,[28] Yu.Galaktionov,[29,16] S.N.Ganguli,[11] P.Garcia-Abia,[6] M.Gataullin,[33] S.S.Gau,[13] S.Gentile,[37] N.Gheordanescu,[14] S.Giagu,[37] S.Goldfarb,[23] J.Goldstein,[12] Z.F.Gong,[21] A.Gougas,[5] G.Gratta,[33] M.W.Gruenewald,[9] R.van Gulik,[2] V.K.Gupta,[36] A.Gurtu,[11] L.J.Gutay,[46] D.Haas,[6] B.Hartmann,[1] A.Hasan,[31] D.Hatzifotiadou,[10] T.Hebbeker,[9] A.Hervé,[18] P.Hidas,[15] J.Hirschfelder,[35] W.C.van Hoek,[32] H.Hofer,[49] H.Hoorani,[35] S.R.Hou,[51] G.Hu,[5] I.Iashvili,[48] B.N.Jin,[8] L.W.Jones,[3] P.de Jong,[18] I.Josa-Mutuberria,[27] R.A.Khan,[19] D.Kamrad,[48] J.S.Kapustinsky,[25] M.Kaur,[19,◇] M.N.Kienzle-Focacci,[20] D.Kim,[37] D.H.Kim,[43] J.K.Kim,[43] S.C.Kim,[43] W.W.Kinnison,[25] A.Kirkby,[33] D.Kirkby,[33] J.Kirkby,[18] D.Kiss,[15] W.Kittel,[32] A.Klimentov,[16,29] A.C.König,[32] A.Kopp,[48] I.Korolko,[29] V.Koutsenko,[16,29] R.W.Kraemer,[35] W.Krenz,[1] A.Kunin,[16,29] P.Lacentre,[48,♮,♯] P.Ladron de Guevara,[27] I.Laktineh,[26] G.Landi,[17] C.Lapoint,[16] K.Lassila-Perini,[49] P.Laurikainen,[22] A.Lavorato,[39] M.Lebeau,[18] A.Lebedev,[16] P.Lebrun,[26] P.Lecomte,[49] P.Lecoq,[18] P.Le Coultre,[49] H.J.Lee,[9] J.M.Le Goff,[18] R.Leiste,[48] E.Leonardi,[37] P.Levtchenko,[38] C.Li,[21] C.H.Lin,[51] W.T.Lin,[51] F.L.Linde,[2,18] L.Lista,[30] Z.A.Liu,[8] W.Lohmann,[48] E.Longo,[37] W.Lu,[33] Y.S.Lu,[8] K.Lübelsmeyer,[1] C.Luci,[18,37] D.Luckey,[16] L.Luminari,[37] W.Lustermann,[49] W.G.Ma,[21] M.Maity,[11] G.Majumder,[11] L.Malgeri,[18] A.Malinin,[29] C.Maña,[27] D.Mangeol,[32] P.Marchesini,[49] G.Marian,[44,¶] A.Marin,[12] J.P.Martin,[26] F.Marzano,[37] G.G.G.Massaro,[2] K.Mazumdar,[11] R.R.McNeil,[7] S.Mele,[18] L.Merola,[30] M.Meschini,[17] W.J.Metzger,[32] M.von der Mey,[1] D.Migani,[10] A.Mihul,[14] A.J.W.van Mil,[32] H.Milcent,[18] G.Mirabelli,[37] J.Mnich,[18] P.Molnar,[9] B.Monteleoni,[17] R.Moore,[3] T.Moulik,[11] R.Mount,[33] G.S.Muanza,[26] F.Muheim,[20] A.J.M.Muijs,[2] S.Nahn,[16] M.Napolitano,[30] F.Nessi-Tedaldi,[49] H.Newman,[33] T.Niessen,[1] A.Nippe,[23] A.Nisati,[37] H.Nowak,[48] Y.D.Oh,[43] G.Organtini,[37] R.Ostonen,[22] C.Palomares,[27] D.Pandoulas,[1] S.Paoletti,[37,18] P.Paolucci,[30] H.K.Park,[35] I.H.Park,[43] G.Pascale,[37] G.Passaleva,[18] S.Patricelli,[30] T.Paul,[13] M.Pauluzzi,[34] C.Paus,[18] F.Pauss,[49] D.Peach,[18] M.Pedace,[37] Y.J.Pei,[1] S.Pensotti,[28] D.Perret-Gallix,[4] B.Petersen,[32] S.Petrak,[9] A.Pevsner,[5] D.Piccolo,[30] M.Pieri,[17] P.A.Piroué,[36] E.Pistolesi,[28] V.Plyaskin,[29] M.Pohl,[49] V.Pojidaev,[29,17] H.Postema,[16] J.Pothier,[18] N.Produit,[20] D.Prokofiev,[38] J.Quartieri,[39] G.Rahal-Callot,[49] N.Raja,[11] P.G.Rancoita,[28] M.Rattaggi,[28] G.Raven,[40] P.Razis,[31] D.Ren,[49] M.Rescigno,[37] S.Reucroft,[13] T.van Rhee,[45] S.Riemann,[48] K.Riles,[3] A.Robohm,[49] J.Rodin,[44] B.P.Roe,[3] L.Romero,[27] S.Rosier-Lees,[4] S.Roth,[1] J.A.Rubio,[18] D.Ruschmeier,[9] H.Rykaczewski,[49] S.Sakar,[37] J.Salicio,[18] E.Sanchez,[27] M.P.Sanders,[32] M.E.Sarakinos,[22] C.Schäfer,[1] V.Schegelsky,[38] S.Schmidt-Kaerst,[1] D.Schmitz,[1] N.Scholz,[49] H.Schopper,[50] D.J.Schotanus,[32] J.Schwenke,[1] G.Schwering,[1] C.Sciacca,[30] D.Sciarrino,[20] L.Servoli,[34] S.Shevchenko,[33] N.Shivarov,[42] V.Shoutko,[29] J.Shukla,[25] E.Shumilov,[29] A.Shvorob,[33] T.Siedenburg,[1] D.Son,[43] B.Smith,[16] P.Spillantini,[17] M.Steuer,[16] D.P.Stickland,[36] A.Stone,[7] H.Stone,[36] B.Stoyanov,[42] A.Straessner,[1] K.Sudhakar,[11] G.Sultanov,[19] L.Z.Sun,[21] G.F.Susinno,[20] H.Suter,[49] J.D.Swain,[19] Z.Szillasi,[44,¶] X.W.Tang,[8] L.Tauscher,[6] L.Taylor,[13] C.Timmermans,[32] Samuel C.C.Ting,[16] S.M.Ting,[16] S.C.Tonwar,[11] J.Tóth,[15] C.Tully,[36] K.L.Tung,[8] Y.Uchida,[16] J.Ulbricht,[49] E.Valente,[37] G.Vesztergombi,[15] I.Vetlitsky,[29] G.Viertel,[49] S.Villa,[13] M.Vivargent,[4] S.Vlachos,[6] H.Vogel,[35] H.Vogt,[48] I.Vorobiev,[18,29] A.A.Vorobyov,[38] A.Vorvolakos,[31] M.Wadhwa,[6] W.Wallraff,[1] J.C.Wang,[16] X.L.Wang,[21] Z.M.Wang,[21] A.Weber,[1] S.X.Wu,[16] S.Wynhoff,[1] J.Xu,[12] Z.Z.Xu,[21] B.Z.Yang,[21] C.G.Yang,[8] H.J.Yang,[8] M.Yang,[8] J.B.Ye,[21] S.C.Yeh,[52] J.M.You,[35] An.Zalite,[38] Yu.Zalite,[38] P.Zemp,[49] Y.Zeng,[1] Z.P.Zhang,[21] B.Zhou,[12] G.Y.Zhu,[8] R.Y.Zhu,[33] A.Zichichi,[10,18,19] F.Ziegler,[48] G.Zilizi,[44,¶]

1 I. Physikalisches Institut, RWTH, D-52056 Aachen, FRG[§]
III. Physikalisches Institut, RWTH, D-52056 Aachen, FRG[§]
2 National Institute for High Energy Physics, NIKHEF, and University of Amsterdam, NL-1009 DB Amsterdam, The Netherlands
3 University of Michigan, Ann Arbor, MI 48109, USA
4 Laboratoire d'Annecy-le-Vieux de Physique des Particules, LAPP,IN2P3-CNRS, BP 110, F-74941 Annecy-le-Vieux CEDEX, France
5 Johns Hopkins University, Baltimore, MD 21218, USA
6 Institute of Physics, University of Basel, CH-4056 Basel, Switzerland
7 Louisiana State University, Baton Rouge, LA 70803, USA
8 Institute of High Energy Physics, IHEP, 100039 Beijing, China[△]
9 Humboldt University, D-10099 Berlin, FRG[§]
10 University of Bologna and INFN-Sezione di Bologna, I-40126 Bologna, Italy
11 Tata Institute of Fundamental Research, Bombay 400 005, India
12 Boston University, Boston, MA 02215, USA
13 Northeastern University, Boston, MA 02115, USA
14 Institute of Atomic Physics and University of Bucharest, R-76900 Bucharest, Romania
15 Central Research Institute for Physics of the Hungarian Academy of Sciences, H-1525 Budapest 114, Hungary[‡]
16 Massachusetts Institute of Technology, Cambridge, MA 02139, USA
17 INFN Sezione di Firenze and University of Florence, I-50125 Florence, Italy
18 European Laboratory for Particle Physics, CERN, CH-1211 Geneva 23, Switzerland
19 World Laboratory, FBLJA Project, CH-1211 Geneva 23, Switzerland
20 University of Geneva, CH-1211 Geneva 4, Switzerland
21 Chinese University of Science and Technology, USTC, Hefei, Anhui 230 029, China[△]
22 SEFT, Research Institute for High Energy Physics, P.O. Box 9, SF-00014 Helsinki, Finland
23 University of Lausanne, CH-1015 Lausanne, Switzerland
24 INFN-Sezione di Lecce and Universitá Degli Studi di Lecce, I-73100 Lecce, Italy
25 Los Alamos National Laboratory, Los Alamos, NM 87544, USA
26 Institut de Physique Nucléaire de Lyon, IN2P3-CNRS,Université Claude Bernard, F-69622 Villeurbanne, France
27 Centro de Investigaciones Energeticas, Medioambientales y Tecnologicas, CIEMAT, E-28040 Madrid, Spain[♭]
28 INFN-Sezione di Milano, I-20133 Milan, Italy
29 Institute of Theoretical and Experimental Physics, ITEP, Moscow, Russia
30 INFN-Sezione di Napoli and University of Naples, I-80125 Naples, Italy
31 Department of Natural Sciences, University of Cyprus, Nicosia, Cyprus
32 University of Nijmegen and NIKHEF, NL-6525 ED Nijmegen, The Netherlands
33 California Institute of Technology, Pasadena, CA 91125, USA
34 INFN-Sezione di Perugia and Universitá Degli Studi di Perugia, I-06100 Perugia, Italy
35 Carnegie Mellon University, Pittsburgh, PA 15213, USA
36 Princeton University, Princeton, NJ 08544, USA
37 INFN-Sezione di Roma and University of Rome, "La Sapienza", I-00185 Rome, Italy
38 Nuclear Physics Institute, St. Petersburg, Russia
39 University and INFN, Salerno, I-84100 Salerno, Italy
40 University of California, San Diego, CA 92093, USA
41 Dept. de Fisica de Particulas Elementales, Univ. de Santiago, E-15706 Santiago de Compostela, Spain
42 Bulgarian Academy of Sciences, Central Lab. of Mechatronics and Instrumentation, BU-1113 Sofia, Bulgaria
43 Center for High Energy Physics, Adv. Inst. of Sciences and Technology, 305-701 Taejon, Republic of Korea
44 University of Alabama, Tuscaloosa, AL 35486, USA
45 Utrecht University and NIKHEF, NL-3584 CB Utrecht, The Netherlands
46 Purdue University, West Lafayette, IN 47907, USA
47 Paul Scherrer Institut, PSI, CH-5232 Villigen, Switzerland
48 DESY-Institut für Hochenergiephysik, D-15738 Zeuthen, FRG
49 Eidgenössische Technische Hochschule, ETH Zürich, CH-8093 Zürich, Switzerland
50 University of Hamburg, D-22761 Hamburg, FRG
51 National Central University, Chung-Li, Taiwan, China
52 Department of Physics, National Tsing Hua University, Taiwan, China
§ Supported by the German Bundesministerium für Bildung, Wissenschaft, Forschung und Technologie
‡ Supported by the Hungarian OTKA fund under contract numbers T019181, F023259 and T024011.
¶ Also supported by the Hungarian OTKA fund under contract numbers T22238 and T026178.
♭ Supported also by the Comisión Interministerial de Ciencia y Tecnología.
♯ Also supported by CONICET and Universidad Nacional de La Plata, CC 67, 1900 La Plata, Argentina.
♮ Supported by Deutscher Akademischer Austauschdienst.
♢ Also supported by Panjab University, Chandigarh-160014, India.
△ Supported by the National Natural Science Foundation of China.

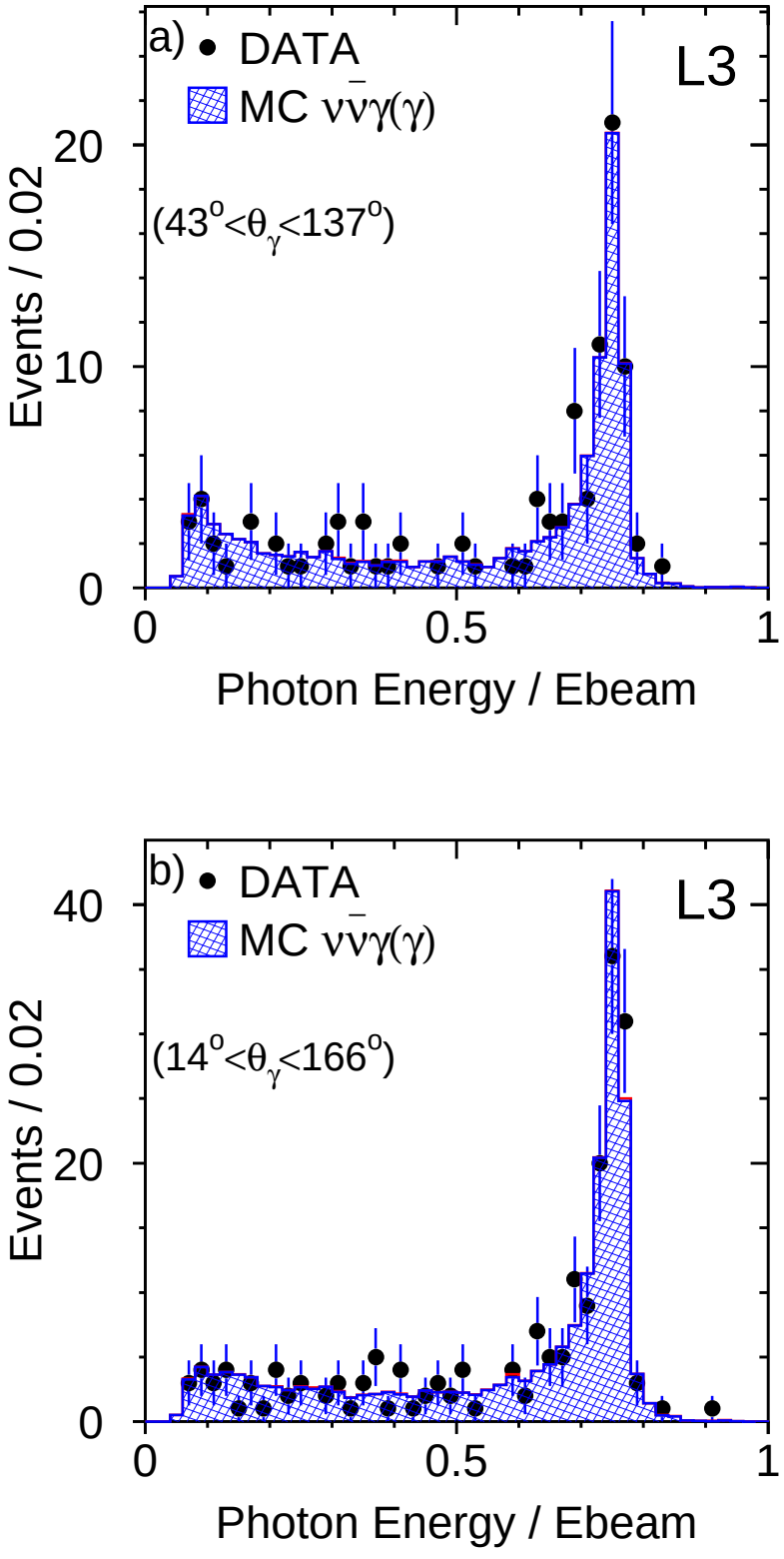

Figure 1: a) Observed energy spectrum of the highest energy photon, normalized to the beam energy, for single and multi-photon events at 183 GeV in the barrel region. b) The same distribution when the end-caps are also included.

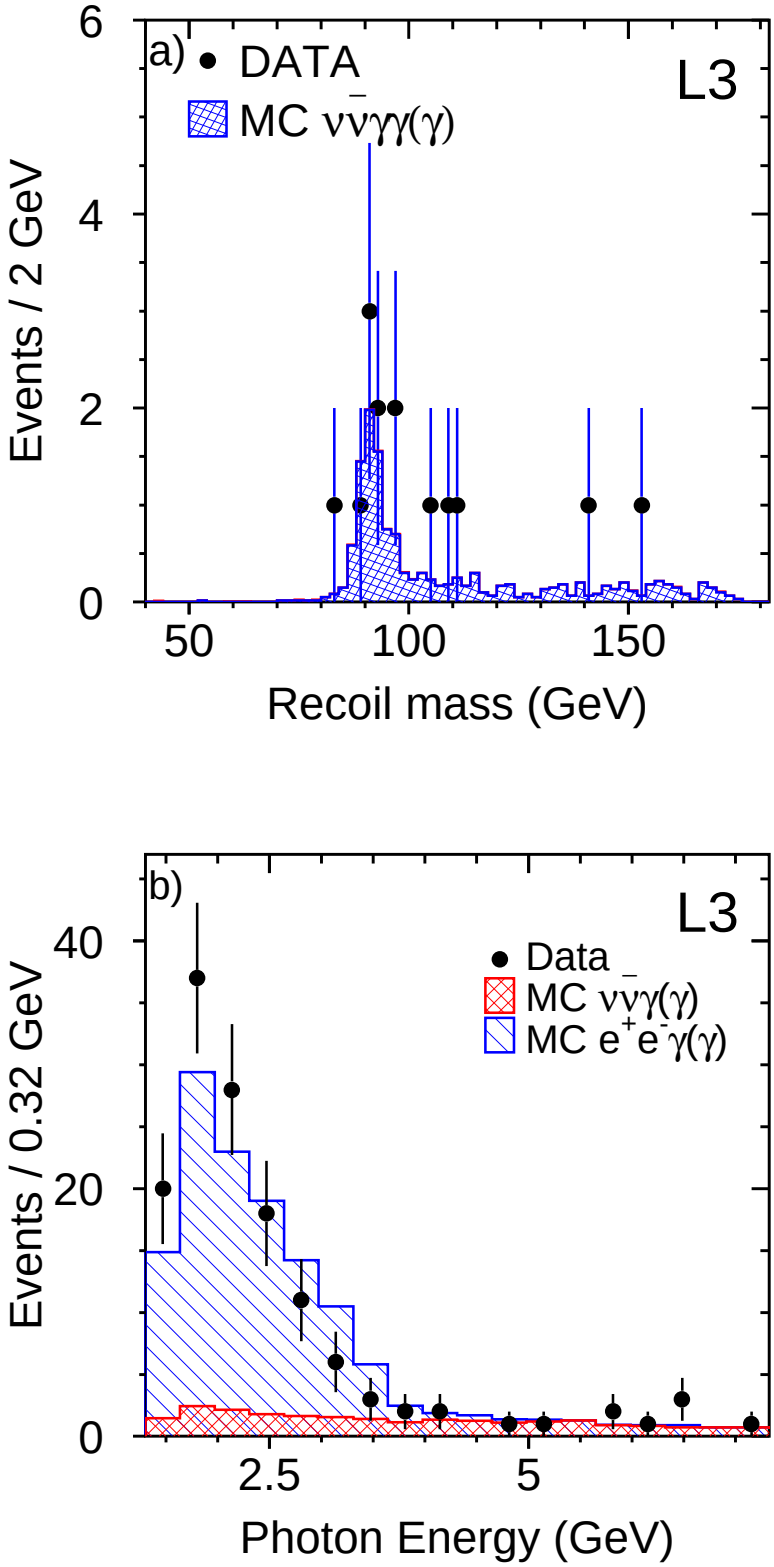

Figure 2: a) Recoil mass distribution for the two photon sample. b) Energy spectrum of the selected low energy single photon events in the barrel region.

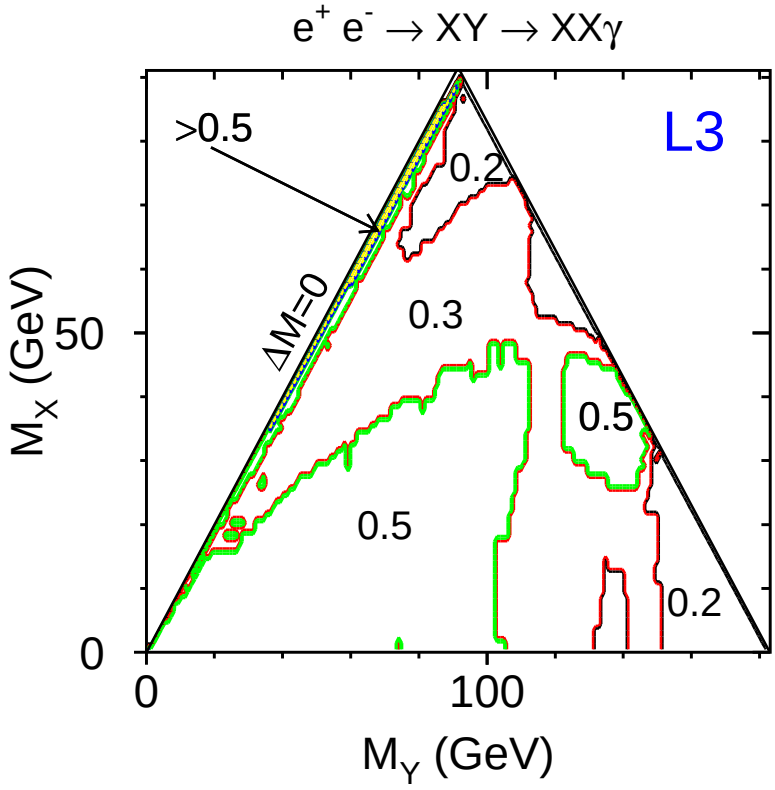

Figure 3: Upper limits at 95% C.L. on the production cross section in pb, for the process $e^+e^- \to XY \to XX\gamma$.

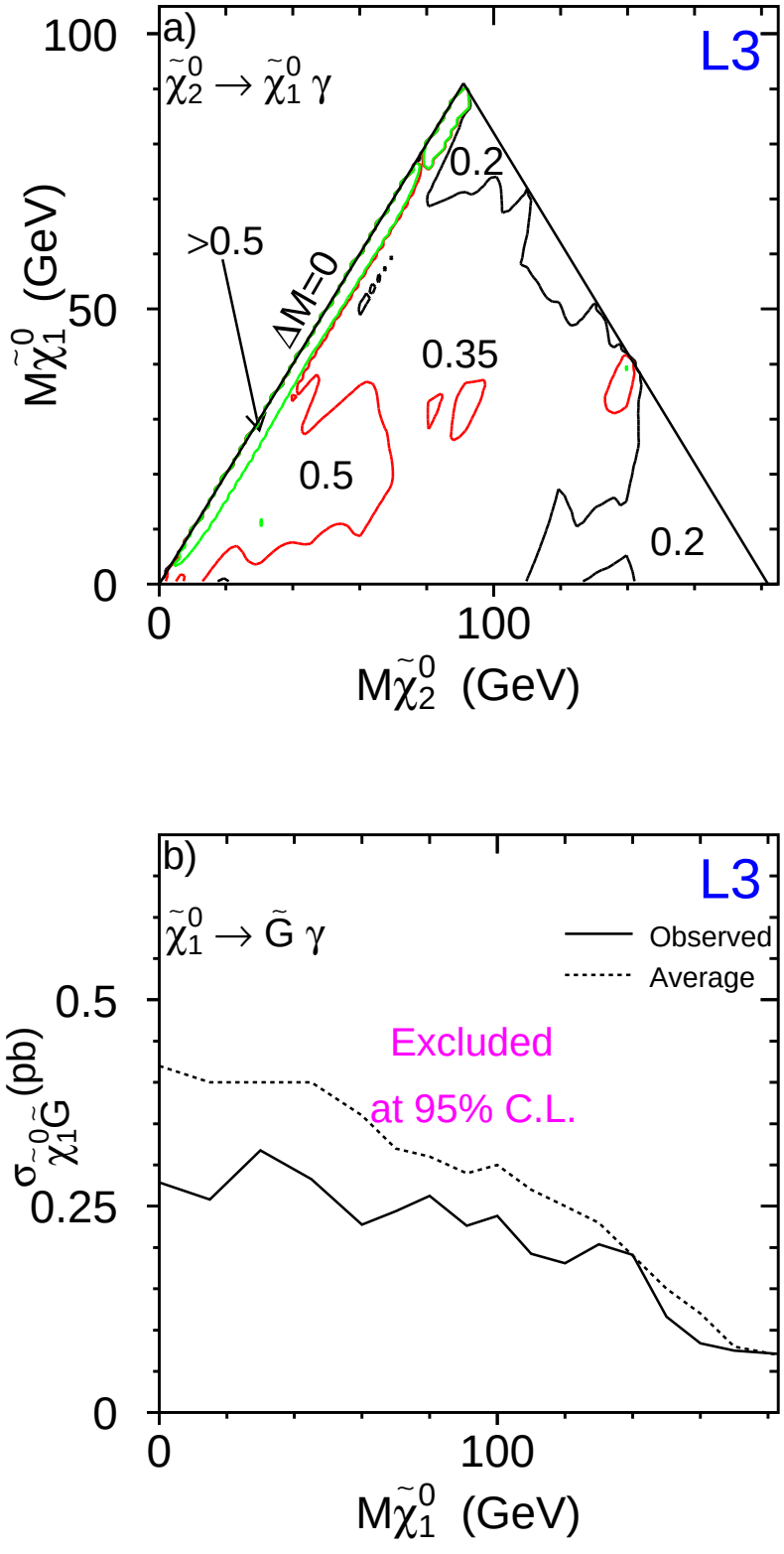

Figure 4: a) Upper limits at 95% C.L. on the production cross section in pb, for the process $e^+e^- \to \tilde{\chi}_2^0\tilde{\chi}_1^0 \to \tilde{\chi}_1^0\tilde{\chi}_1^0\gamma$. b) Upper limits on the production cross section for the process $e^+e^- \to \tilde{G}\tilde{\chi}_1^0 \to \tilde{G}\tilde{G}\gamma$. The dashed line shows the average limit obtained with Monte Carlo experiments with background only.

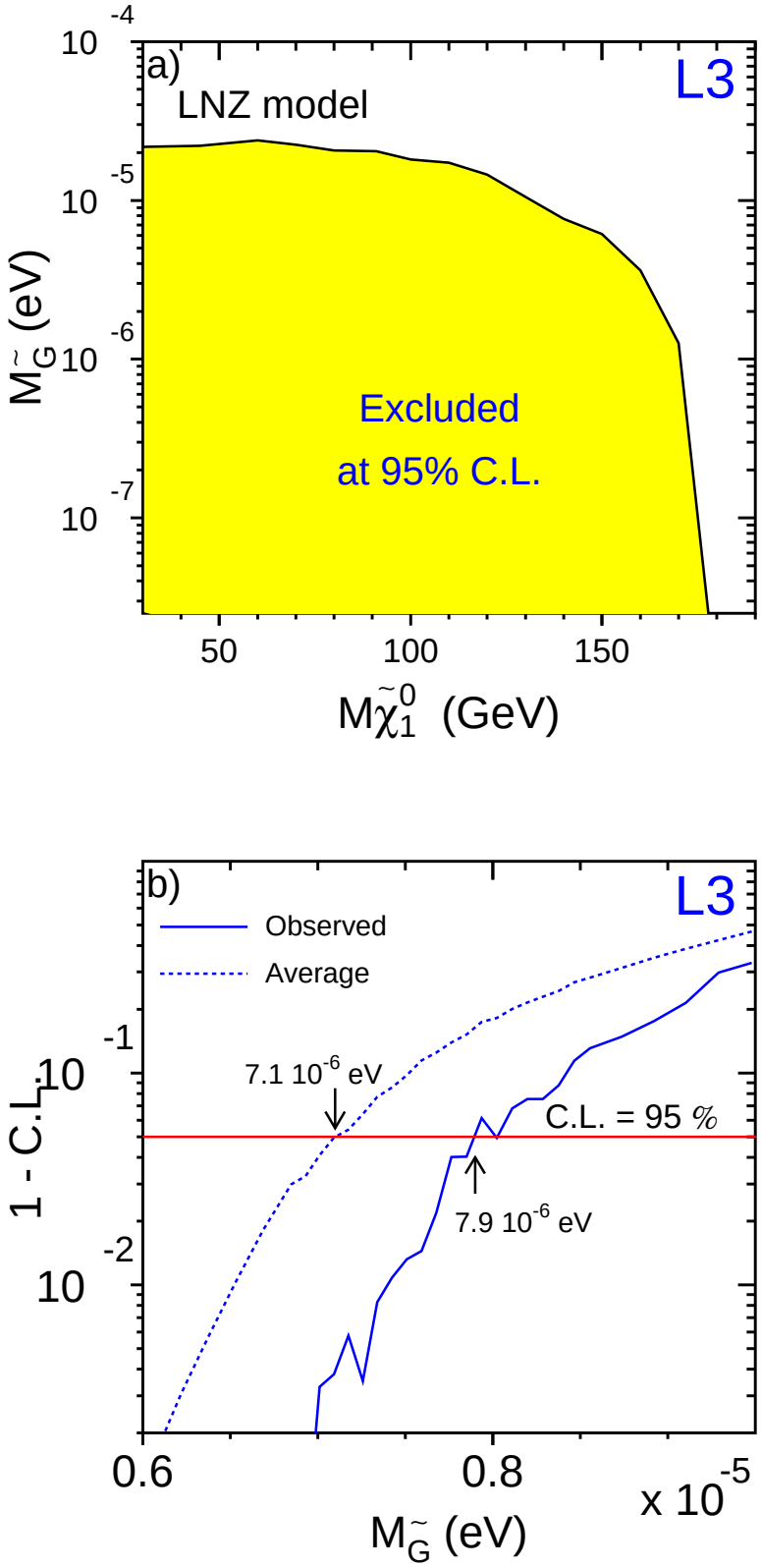

Figure 5: a) Excluded region at 95% C.L., in the LNZ model, in the plane $M_{\tilde{G}} - M_{\tilde{\chi}_1^0}$. b) Confidence level for exclusion as a function of the gravitino mass (solid line). The dashed line shows the average confidence level obtained with Monte Carlo experiments with background only.

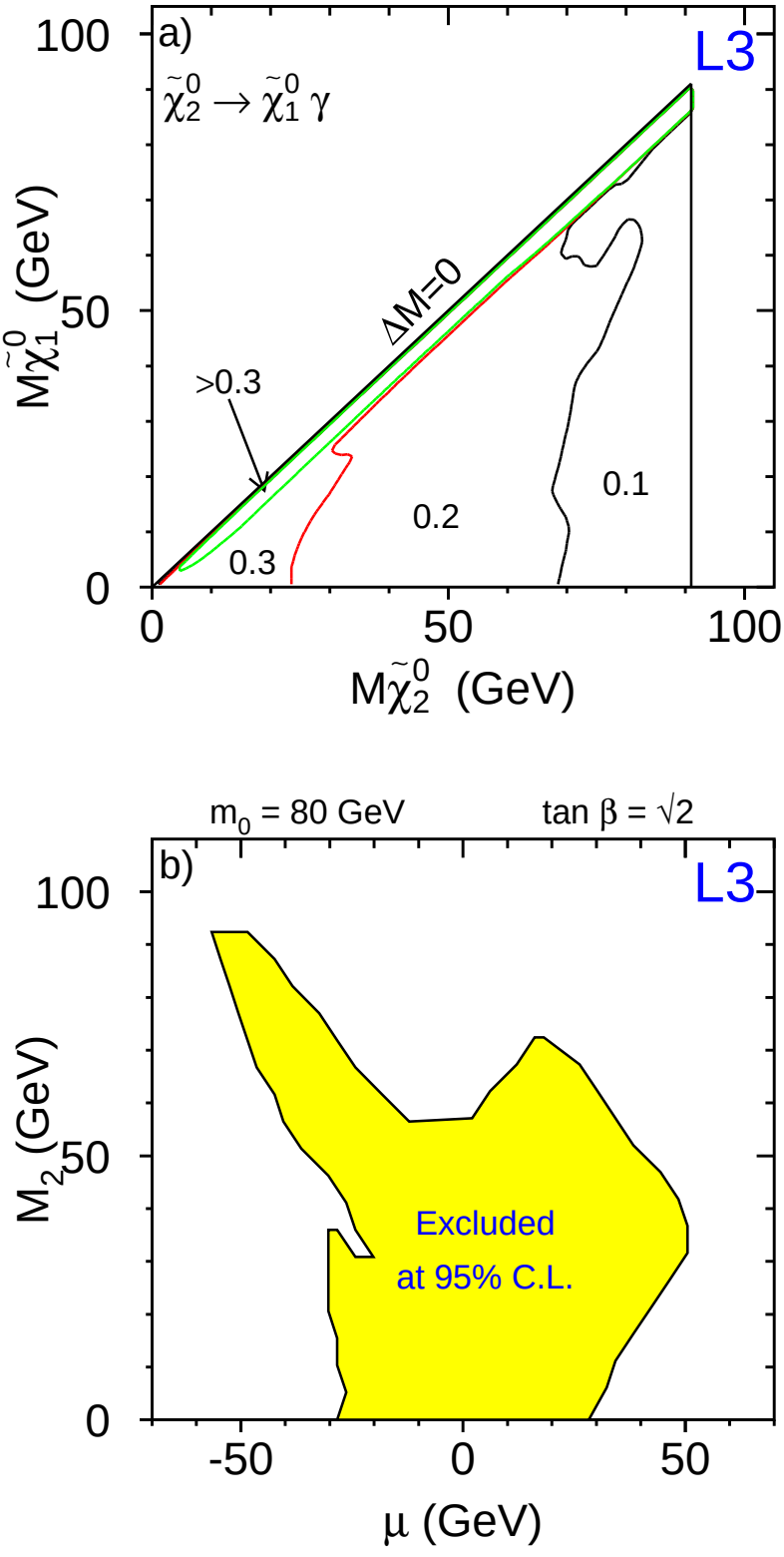

Figure 6: a) Upper limits at 95% C.L. on the production cross section in pb, for the process $e^+e^- \rightarrow \tilde{\chi}_2^0\tilde{\chi}_2^0 \rightarrow \tilde{\chi}_1^0\tilde{\chi}_1^0\gamma\gamma$. b) Excluded region in the $M_2 - \mu$ plane for $\tan\beta = \sqrt{2}$ and $m_0 = 80$ GeV, in the heavy gravitino scenario.

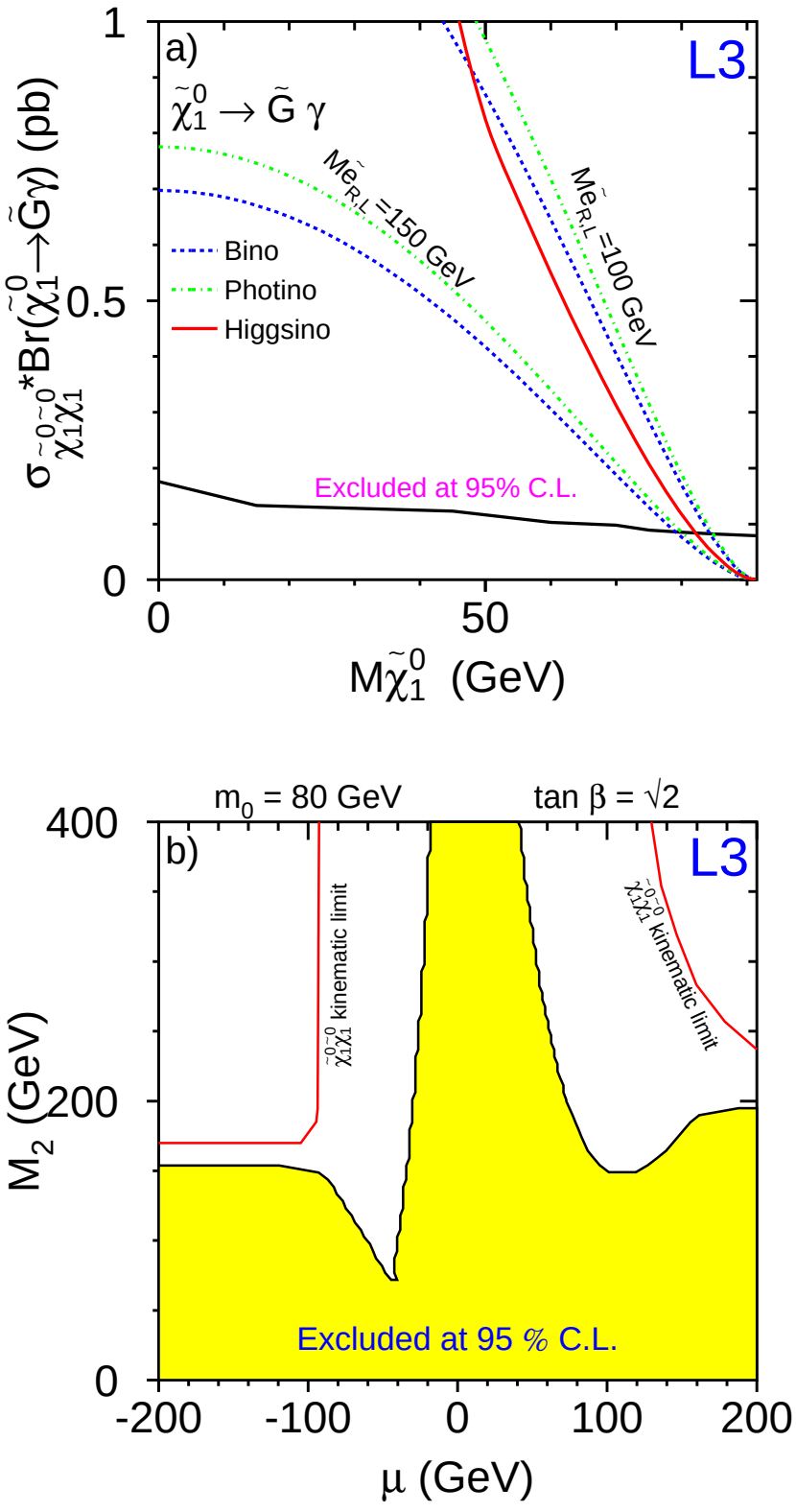

Figure 7: a) Upper limit at 95% C.L. on the cross section for the process $e^+e^- \to \tilde{\chi}_1^0\tilde{\chi}_1^0 \to \tilde{G}\tilde{G}\gamma\gamma$. The theoretical predictions for three extreme cases of $\tilde{\chi}_1^0$ composition and for two different scalar electron masses are also shown. b) Excluded region in the $M_2 - \mu$ plane for $\tan\beta = \sqrt{2}$ and $m_0 = 80$ GeV, in the light gravitino scenario.

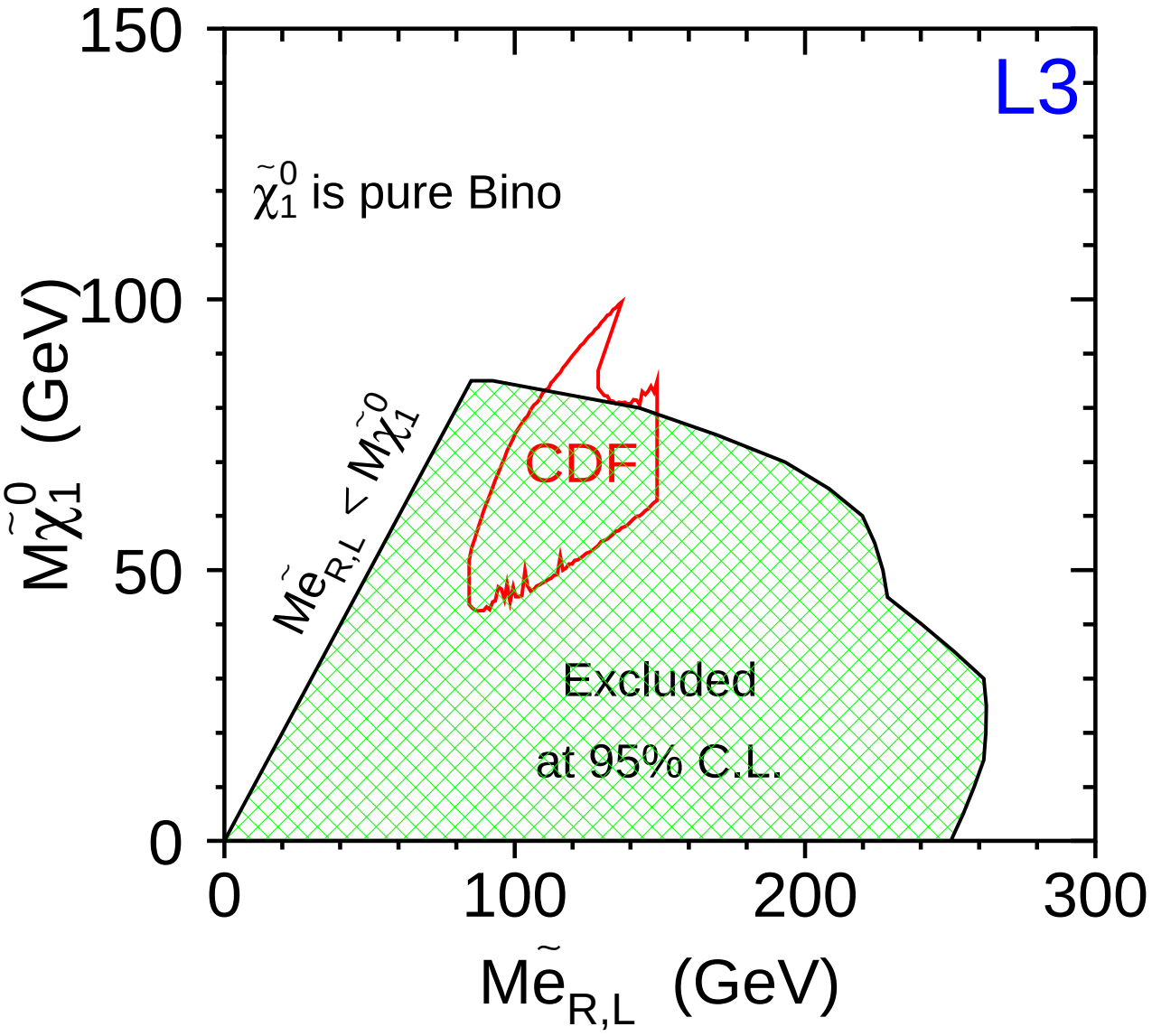

Figure 8: Excluded region in the GMSB model compared to the region consistent with the supersymmetric interpretation of the CDF event in the so-called scalar electron scenario.